Chin. Phys. B Vol. 25, No. 9 (2016) 097307

RAPID COMMUNICATION

Carrier transport in III–V quantum-dot structures for solar cells or photodetectors*

Wenqi Wang(王文奇)†, Lu Wang(王禄)†, Yang Jiang(江洋), Ziguang Ma(马紫光), Ling Sun(孙令), Jie Liu(刘洁), Qingling Sun(孙庆灵), Bin Zhao(赵斌), Wenxin Wang(王文新), Wuming Liu(刘伍明), Haiqiang Jia(贾海强), and Hong Chen(陈弘)‡

Key Laboratory for Renewable Energy, Beijing Key Laboratory for New Energy Materials and Devices, Beijing National Laboratory for Condensed Matter Physics, Institute of Physics, Chinese Academy of Sciences, Beijing 100190, *China*

(Received 15 July 2016; published online 2 August 2016)

According to the well-established light-to-electricity conversion theory, resonant excited carriers in the quantum dots will relax to the ground states and cannot escape from the quantum dots to form photocurrent, which have been observed in quantum dots without a p–n junction at an external bias. Here, we experimentally observed more than 88% of the resonantly excited photo carriers escaping from InAs quantum dots embedded in a short-circuited p–n junction to form photocurrent. The phenomenon cannot be explained by thermionic emission, tunneling process, and intermediate-band theories. A new mechanism is suggested that the photo carriers escape directly from the quantum dots to form photocurrent rather than relax to the ground state of quantum dots induced by a p–n junction. The finding is important for understanding the low-dimensional semiconductor physics and applications in solar cells and photodiode detectors.

Keywords: quantum dots, electronic transport, p–n junctions, photoluminescence

PACS: 73.21.La, 73.63.–b, 73.40.Kp, 78.55.–m **DOI:** 10.1088/1674-1056/25/9/097307

1. Introduction

Practically, most photovoltaic devices including solar cells and photovoltaic detectors incorporate a p–n junction in a semiconductor utilizing photovoltaic effect to convert light into electricity.[1–3] Large optical absorption coefficients and great carrier extraction capability are conductive to solar cells[4] and photovoltaic devices.[5] In order to fully absorb the light, solar cells and photodiode detectors mainly make use of bulk materials.[6] Furthermore, to obtain high crystalline quality, low-dimensional semiconductors have been applied in solar cells[7,8] and photovoltaic detectors.[9]

Recently, quantum dots (QDs) have garnered extensive interest for applications in optoelectronic devices because of their strong zero-dimensional confinement effects with a δ-function density of states.[10–12] These characteristics make the QDs to form their distinct quasi-Fermi level and to restrict photo-generating carriers to the ground energy level.[13,14] Consequently, without additional excitation, carriers in the quantum restriction level cannot escape to external circuit,[15,16] so QDs as an intermediate-band have been suggested to utilizing low energy photon in the solar spectrum.[17,18] The principle is that one photon pumps an electron from the valence band (VB) to conduction band of a QD, namely intermediate band (IB), while the second one pumps an electron from the IB to the conduction band (CB) of the barrier.[16,19] which can produce photocurrent from photon absorption by QDs.[20] However, all investigations have failed to preserve the open-circuit voltage of an IBSC compared to that of a standard solar cell,[16,19,21] which is explained by tunneling and thermal emission processes.[22,23]

It is reported that the mechanism of IBSC has been confirmed when the photocurrent increases under two sub-band-gap energy lasers shone on IBSC.[24,25] However, the experimental results cannot rule out the possibility that the photocurrent separately comes from the VB to IB transition or IB to CB transition,[26,27] respectively. Namely, it cannot confirm that the increase of photocurrent is caused by two successive jumps. Thus, the carrier transport process is not clear so far. In order to solve this problem, we use only one laser to pump an electron from the VB of a QD to its CB, then find that a p–n junction induces the most of photo-excited carriers to directly escape from the QDs to generate the photocurrent rather than relax to the ground state under the short-circuit condition. The results cannot be well explained by the current light-to-electricity conversion theory.[20]

*Project supported by the National Natural Science Foundation of China (Grant Nos. 11574362, 61210014, 11374340, and 11474205) and the Innovative Clean-Energy Research and Application Program of Beijing Municipal Science and Technology Commission, China (Grant No. Z151100003515001).

†These authors contributed equally to this work.

‡Corresponding author. E-mail: hchen@iphy.ac.cn

© 2016 Chinese Physical Society and IOP Publishing Ltd

2. Experiment

Two sample structures with n–n and p–n structures (Fig. 1) were grown by molecular beam epitaxy on a GaAs substrate. Experimental details are shown in Appendix A. Sample A (Fig. 1(a)) consisted of ten layers of InAs QDs inside a GaAs host without a p–n junction; Sample B (Fig. 1(b)) was identical to Sample A except that it had a p–n junction. Figure 1(c) shows the AFM observation of typical InAs QDs. The InAs QDs exhibited a well-defined shape with an areal density of 2.2×10^{10} cm^{-2}. Judging from the individual QD image, the typical diameter was approximately 20 nm, and the effective dots height was about 6 nm. In our observation, no giant dot accrued in the scale of AFM image. After the epitaxy, two samples were fabricated into 2 mm×2 mm chips to investigate their optoelectronic characteristics. In this experiment, the excitation source was a semiconductor laser with a wavelength of 915 nm, the corresponding photon energy of 1.35 eV that lies between the band gap of the GaAs (1.519 eV) and that (0.41 eV) of InAs QDs; therefore, the photo-carriers responsible for excitation were exclusively generated and restricted in the QDs.[28] Since the absorption wavelength from the CB of a QD to the CB of the GaAs barrier was ranging from 2 μm to 6 μm,[29,30] the photocurrent generating due to IB to CB transition could be ruled out.

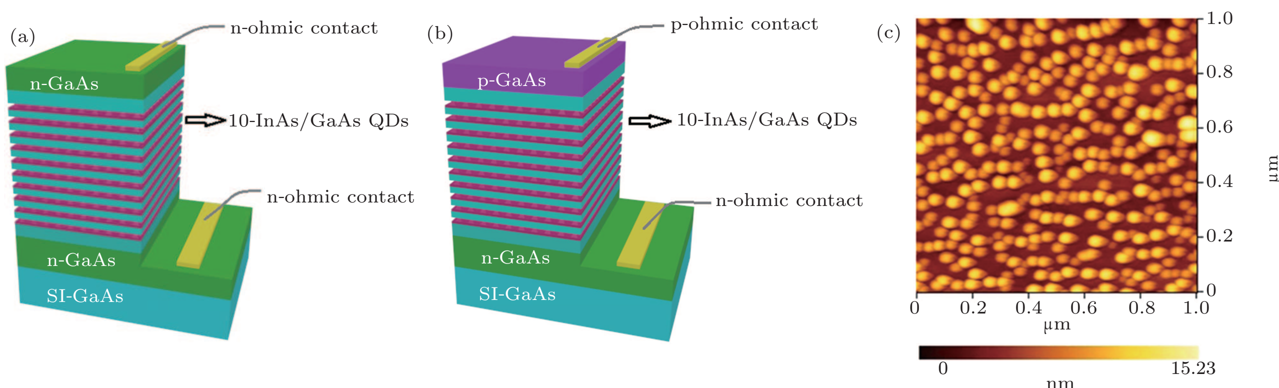

Fig. 1. (color online) Schematics of two different ten-layer QD structures. (a) Schematic of Sample A. The InAs/GaAs multilayer dots are the active region and are sandwiched between n-type and n-type GaAs; each of them consists of 2.2-ML InAs quantum dots and 50-nm GaAs barrier layer. (b) Schematic of Sample B. It is deposited similarly, except that the n-GaAs is substituted by an equal thickness of p-GaAs. (c) Atomic force microscope (AFM) image of InAs quantum dots. The scan area is 1 μm×1 μm.

3. Results and discussion

The photoluminescence (PL) spectra of Sample A were measured at 150 K under the open-circuit condition and with a 0.7-V bias to provide an external electrical field (Fig. 2(a)). The QD PL peak is fitted by Gaussian function and the FWHM is 72.6 meV resulting from the inhomogeneity of the QDs, which agree with these reported before.[31] The PL intensity under the 0.7-V bias is reduced by 7.3% compared with that

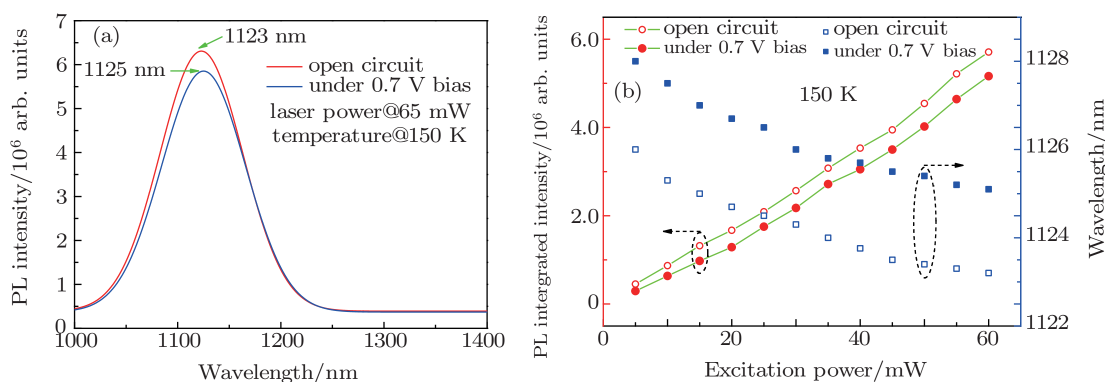

Fig. 2. (color online) The photoluminescence (PL) spectra of Sample A under resonant excitation at the wavelength of 915 nm, at 150 K, and under an incident light with a power of 65 mW. (a) The PL spectra of Sample A measured for the open-circuit condition with a 0.7-V bias using a laser power excitation of 65 mW. The PL intensity decreases by 7.3% when a 0.7-V bias is applied on Sample A. The PL peak position of Sample A for the open-circuit condition is 1123 nm and is red-shifted to 1125 nm when a 0.7-V bias is applied. This red shift arises from the energy band slant under the applied electric field. (b) Excitation-power-dependent PL integrated intensity and peak wavelength of the PL spectrum for the open-circuit and 0.7-V bias conditions. The percentage of the PL intensity decreases from 90% to 65% with the decrease of the light power. The PL peak position is blue-shifted from 1126 nm to 1123.2 nm and from 1128 nm to 1125.1 nm for the open-circuit and 0.7-V bias conditions, respectively. The PL peak positions are blue-shifted when the laser power is increased because of the band-filling effect.

under the open-circuit condition; the peak shift resulting from the quantum-confined Stark effect confirms that a bias has been applied to the QDs.[32] Moreover, the excitation-power-dependent PL was measured to confirm these results (Fig. 2(b)). The PL intensity of Sample A linearly increases with the increase of the power of the incident light. These results agree with those in the previous literature.[33] The ratio of the integrated PL intensity under 0.7-V bias to the open-circuit one decreases from 90% to 65% as the light power decreases.

The resonant PL spectra of Sample B were measured at 150 K under open- and short-circuit conditions (Fig. 3(a)), a clear difference is observed in the PL intensity under the two conditions. The integrated PL intensity in the short-circuit condition is reduced to approximately 12% of the intensity in the open-circuit. The reduction of the PL intensity indicates that approximately 88% of photocarriers did not participate in the recombination in QDs anymore.

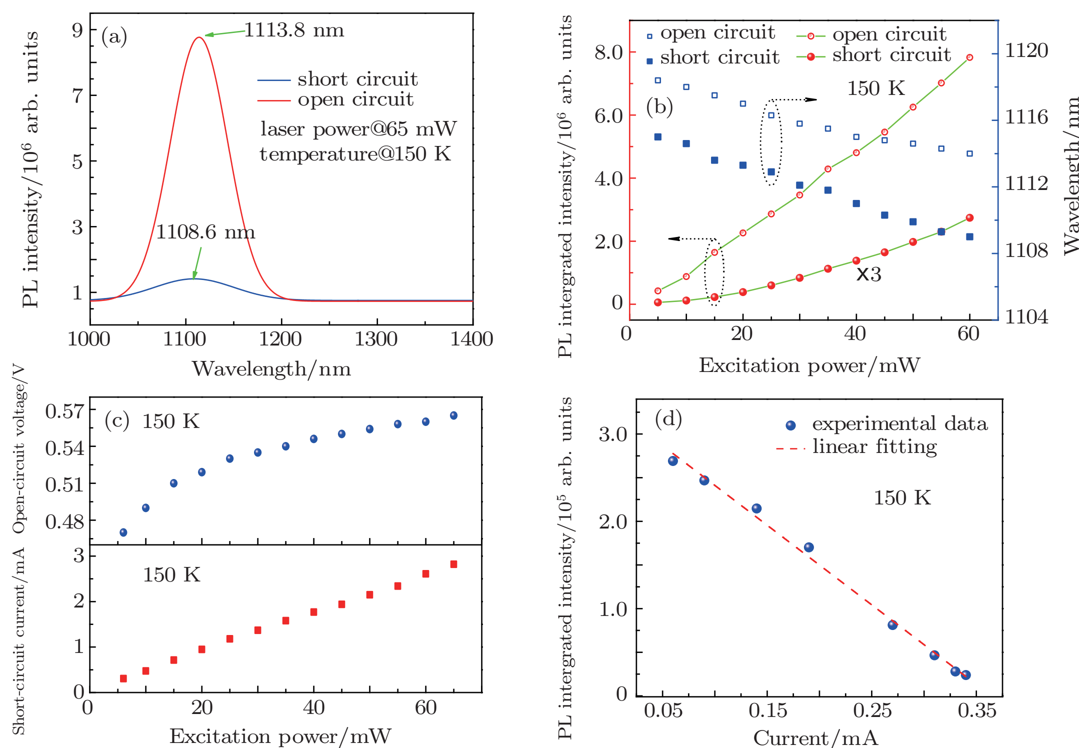

Fig. 3. (color online) The PL spectra and light-to-electricity conversion results of Sample B for the resonant excitation by light with a wavelength of 915 nm under an incident light with a power of 65 mW. (a) PL spectra of Sample A collected under the short- and open-circuit conditions. The PL integrated intensity is reduced by 88% when the circuit is changed from open to short. Meanwhile, the PL peak position is blue-shifted from 1113.8 nm in the open-circuit to 1108.6 nm in the short-circuit. This blue shift in the PL wavelength arises from the change in the Femi energy between the open- and short-circuit conditions. (b) Excitation-power-dependent PL integrated intensity and peak position variation under open- and short-circuit conditions. The ratio between the integrated PL intensity under the short-circuit condition to that under the open-circuit condition monotonically increases from 5% to 11.6%. The PL peak position is blue-shifted from 1118.4 nm to 1114 nm under the open-circuit condition and from 1115 nm to 1109 nm under short-circuit condition. The PL peak position is blue-shifted when the laser power increases because of the band-filling effect. (c) Excitation-power-dependent open-circuit voltage (V_{oc}) and short-circuit current (J_{sc}) at 150 K. The J_{sc} is proportional to the incident light intensity, and the V_{oc} is proportional to the logarithm of the incident light intensity. (d) Inversely linearly related circuit current and PL intensity of Sample B under a 65-mW excitation power at 150 K.

To deeply investigate the phenomenon of PL intensity quenching of Sample B under open and short-circuit condition, we varied the incident laser powers from 5 mW to 60 mW to probe the PL spectra (Fig. 3(b)). Under the open-circuit condition, the integrated PL intensity increases linearly with the incident laser powers. However, when Sample B is short-circuited, the integrated PL intensity increases parabolically with the incident laser powers. The ratio of the integrated PL intensity of Sample B in the short-circuit and open-circuit conditions monotonically increases from 5% to 11.6% with the increae of the incident light power, which means that at least 88% resonant excited carriers escape from the QDs to generate an optocurrent. We also measured the optovoltaic effect of Sample B. Figure 3(c) shows the variation of the open-circuit voltage (V_{oc}) and short-circuit current (J_{sc}) for different incident laser powers. In Fig. 3(c), the J_{sc} is linearly proportional to the incident laser powers, whereas the V_{oc} is proportional to the logarithm of the incident laser powersity, consistent with the law of solar cells,[4] which means that the InAs QDs can be used for solar cells and photodetectors.

To clarify the escape pathway of photon-generated carriers, we connected a variable resistor to the circuit to adjust the

circuit current (Fig. 3(d)) to allow PL spectra to be collected for different circuit currents. These experiments reveal a linear relationship between the current and the PL intensity. This result confirms that carriers escaping from the QDs to generate a photocurrent dominate the carrier transport process, which indicates that the QD structure can be applied in solar cells and photodetectors.

The resonant excited photocarriers directly escape from the QDs to generate the photovoltaic effect in Sample B (with a p–n junction) under the short-circuit condition. However, in Sample A (without a p–n junction), the resonant excited photocarriers relax to the ground state and then recombine to emit light under a 0.7-V bias. Because Samples A and B have the same barrier height and thickness, thermionic emission and tunneling processes cannot be used to explain the photo-excited carriers escaping from the quantum dot.[21,22,34,35] It can be deduced that the p–n junction induces the photocarriers escaping from the QDs.

According to the established photon absorption model of QD heterojunction, the basic absorption processes for different values of energy $h\nu$ are shown in Fig. 4(a). When $h\nu > E_g$, an electron–hole pair is created and the excess energy gives them additional kinetic energy, which will be dissipated as heat.[36] In accordance with the above theory, the most of hot photocarriers should relax to the ground state for recombination, only a few photocarriers can escape from the QDs through the thermionic emission process or tunneling process. However, in our experiment we observed more than 88% carriers escaping efficiency of Sample B under the short-circuit condition (Fig. 3(a)). Therefore, we speculate that the free photocarriers in InAs QDs cannot be restricted by barriers and directly drifted to p or n region to form photocurrent, as shown in Fig. 4(b). This is the new mechanism of the carrier transportation processes of QD applications for solar cells and photodetectors.

Firstly, we compared the time of carrier drifting out of the QD and the relaxation time to the ground state to check the possibility that photocarriers can directly escape from the QDs instead of relaxing to the energy level. It has been reported that the time of an electron relaxing to the ground state is approximately several hundred picoseconds.[31] For the short-circuit condition in Sample B (with a p–n junction), the competition between the free excited-state carrier transits over the InAs quantum and relaxes to the ground state, which is critical to account for the experimental phenomenon. The time of the free excited-state carrier transiting over the QD in the depletion region is given by

$$t = \frac{h}{v}, \tag{1}$$

where h is the height of the QDs and v is the drift velocity of the electron or hole. Given that the electron mobilities of InAs and GaAs are mainly larger than 2000 $\mathrm{cm^2 \cdot V^{-1} \cdot s^{-1}}$, the hole mobilities of InAs and GaAs are usually larger than 100 $\mathrm{cm^2 \cdot V^{-1} \cdot s^{-1}}$,[37] and the built-in voltage is larger than 0.5 V, the time of the hole or the electron escaping from the QD is on the order of femtoseconds. Therefore, the free exciting carriers prone to escape from the QD rather than relax to the ground state and emit light.

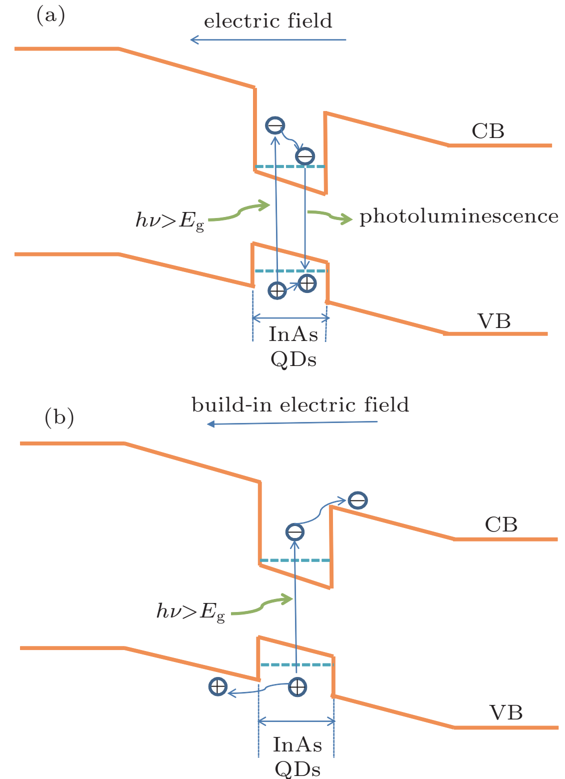

Fig. 4. (color online) Sketch of the photon absorption and carrier transportation processes of InAs quantum dots embedded in GaAs with a p–n junction. (a) Schematic diagram of the established photon absorption and carrier transportation processes. When a photon with energy $h\nu > E_g$ incidents to the sample, the high excited state free electron–hole pair generate, and then relax to the ground state, finally the electron–hole pair recombine and emit a photon. (b) Schematic diagram of the new photon absorption and carrier transportation processes. InAs quantum dots embedded in GaAs with a p–n junction under the short-circuit condition. When a photon with energy $h\nu > E_g$ incidents to the sample, the high excited state free electron–hole pair generate, and then escape directly from InAs quantum dots to external circuit under the driving force of the build-in electric field.

Secondly, we explains why photo-carriers can be extracted from the QDs by a p–n junction rather than by an external voltage bias. For Sample A, when the QD structure is applied with an external bias, the electric-field distribution is nearly uniform at the undoped region. Carrier drift velocity is proportional to the electric field and carrier mobility. Electron mobility is faster than the hole mobility, which leads to the electron drift velocity larger than the hole drift velocity. Furthermore, the electrons drifted from QD region are more

than the holes drifted from QD region. Thus, it will lead to excess holes accumulated in the device and forming a large positive electric field, in turn preventing carriers from escaping. However, for Sample B, in the depletion region, the electric field is a linear function of the distance through the junction and the tendency reverses at the position of abrupt junction. The slope of electric field can be adjusted by changing the dopant concentration of p- or n-type region, respectively. The electric-field distribution in the p–n junction can balance the hole velocity to match the electron velocity, which diminishes the blocking effect of current. The electric-field distribution in the p–n junction facilitates the hole to be extracted and in turn reaches a better electrically neutral condition. The unique characteristic of p–n junction results in continuous carriers escaping from the QDs.

When the incident laser-beam power is 65 mW, we measure that the J_{sc} of Sample B is 2.82 mA at 150 K. The incident-photon-to-current conversion efficiency is calculated as 5.9% under the short-circuit condition. The effective absorption layer is ten layers of InAs QDs, which is approximately 60 nm in total, and the absorption coefficient of the InAs QDs is calculated to be approximately 10^4 cm^{-1}, which far exceeds the theoretical calculation of 100 cm^{-1} for the sample without a p–n junction.[38,39] The absorption coefficient we measured is underestimated because the surface reflection is not considered and the extraction efficiency of the p–n junction is assumed as 100%. Such value is comparable to the absorption coefficient of bulk GaAs near its band gap.[40] Considering the lower density of state and the localized wavefunction of zero-dimensional semiconductor material, it is reasonable to deduce the p–n junction dramatically to enhance the absorption of InAs QDs, which demonstrates that the QDs can be easily used in solar cells and photodetectors.

The results in this study indicate that the final state of the carriers is a free excited state in the QDs within a p–n junction under the short-circuit condition. However, the absorption final state would be a localized ground state, like the QDs under the short-circuit condition in our experiments. Based on the perturbation theory of quantum mechanics, the absorption coefficient is related to the density of states and the wavefunction of the final state of the carriers.[41] The changes of the physical nature increase the absorption coefficient when the QDs within a p–n junction operate under the short-circuit condition. The results deviate from the established theories of solar cells and photodiode detectors, where the absorption coefficient is assumed to be a constant for different conditions.

4. Summary

In summary, we have observed that the most photo-excited carriers escaped from the InAs QDs with a p–n junction under the short-circuit condition, this finding challenges the current light-to-electricity conversion theory. A new mechanics applying InAs QDs incorporate a p–n junction in solar cells and photodetectors is deduced. It is found that the InAs QDs can not only make the design of solar cells more flexible, but also extend the spectrum response range of photodetectors. It is visualized that our mechanism of photo-excited carriers escaping from the QDs can be extended to other materials since the fundamental band-alignment and light absorption process are essentially the same.

Appendix A Experimental details

A.1. Material epitaxy

Ten-layer InAs/GaAs QD n–i–n (Sample A) and p–i–n (Sample B) structures were grown by a solid-source VG-80H molecular beam epitaxy system on semi-insulating GaAs (001) substrates. Ten QD layers with deposition thicknesses of 2.2 ML and grown in the self-assembled Stranski–Krastanov mode were embedded in the middle of a 50-nm-thick intrinsic GaAs space layer. The InAs QDs' deposition rate was 0.02 ML/s and the arsenic pressure was 1×10^{-6} Torr. A 20-s growth interruption was introduced before the InAs QDs were capped to promote the formation of a homogeneous population of QDs. After the deposition of the GaAs buffer and GaAs n$^+$ emitter, the rotated substrate temperature was reduced from 580 °C to 480 °C and maintained at 480 °C until the end of the growth. The Si doping concertation of the n electrodes was $N_D = 3\times10^{18}$ cm^{-3}, and the Si doping concertation of the field damping layer inserted into the structure was $N_D = 6\times10^{17}$ cm^{-3}. The Be doping concentration of the p electrodes was $N_A = 3\times10^{18}$ cm^{-3}, and the Be doping concentration of the field damping layer inserted into the structure was $N_A = 3\times10^{17}$ cm^{-3}.

A.2. Device fabrication

The samples were fabricated by patterning the samples using photolithography and wet etching to achieve mesa isolation and expose the n-GaAs buffer. The mesa area was 4 mm^2. The electrodes of Ti/Au (20/100 nm) were deposited onto the p-GaAs in sequence by electron-beam evaporation. Then, 15/101/26/26/100-nm-thick Ni/Au/Ge/Ni/Au layers were deposited onto the n-GaAs for an n-ohmic contact. A wire bonding system was implemented with Si/Al wire on the electrodes.

A.3. Photoluminescence measurement

The hypothermia photoluminescence intensity of Samples A and B was measured with devices mounted in a closed-loop He-gas cryostat to maintain a stable measurement temperature of 150 K. To achieve non-resonant excitation of the electrons in InAs QDs, a 915-nm 130-mW semiconductor

laser diode was used. The laser incident angle was approximately 30°. A beam chopper with a frequency of 1000 Hz was set up behind the laser. A condenser lens was placed in front of the cryostat to converge the spot. A neutral optical attenuator was used to adjust the excitation power. The PL signal normal to the sample was modulated by a triple-grating 50-cm monochromator prior to the analog lock-in amplifier (Stanford Research Systems model 830) and then detected by an InGaAs detector.

Acknowledgment

We thank the Laboratory of Microfabrication, Institute of Physics, Chinese Academy of Sciences for the fabrication of devices.

References

[1] Goetzbergera A, Heblinga C and Schockb H W 2003 *Mater. Sci. Eng. R* **40** 1
[2] Jenny D A, Loferskr J J and Rappaiport P 1956 *Phys. Rev.* **101** 1208
[3] Chapin D M, Fuller C S and Pearson G L 1954 *J. Appl. Phys.* **25** 676
[4] Nelson J 2003 *The Physics of Solar Cells* (1st edn.) (London: Imperial College Press) pp. 19–37
[5] Rogalski A 2011 *Infrared Detectors* (2nd edn.) (London: Taylor and Francis Group) pp. 295–338
[6] Basu P K 2003 *Theory of Optical Processes in Semiconductors* (2nd edn.) (New York: Oxford University Press) pp. 80–122
[7] Dahal R, Pantha B, Li J, Lin J Y and Jiang H X 2009 *Appl. Phys. Lett.* **94** 063505
[8] Ekins-Daukes N J, Barnham K W J, Connolly J P, Roberts J S, Clark J C, Hill G and Mazzer M 1999 *Appl. Phys. Lett.* **75** 4195
[9] Chiou Y Z, Su Y K, Chang S J, Gong J, Lin Y C, Liu S H and Chang C S 2003 *IEEE J. Quantum Electron.* **39** 681
[10] Yoffe A D 2001 *Adv. Phys.* **50** 1
[11] Bratschitsch R and Leitenstorfer A 2006 *Nat. Mater.* **5** 855
[12] Shields A J 2007 *Nat. Photon.* **1** 215
[13] Bhattacharya P, Ghosh S and Stiff-Roberts A D 2004 *Annu. Rev. Mater. Res.* **34** 1
[14] Reed M A, Randall J N, Aggarwal R J, Matyi R J, Moore T M and Wetsel A E 1988 *Phys. Rev. Lett.* **60** 535
[15] Martí A, Luque A and Nozik A J 2007 *Mrs Bull* **32** 236
[16] Luque A and Martí A 2011 *Nat. Photonics* **5** 137
[17] Bimberg D, Grundmann M and Ledentsov N N 1999 *Quantum Dot Heterostructures* (1st edn.) (New York: Wiley) pp. 1–8
[18] Martí A, Luque A, Stanley C, López N, Cuadra L, Zhou D, Pearson J L and McKee A 2004 *J. Appl. Phys.* **96** 903
[19] Martí A, Luque A and Stanley C 2012 *Nat. Photonics* **6** 146
[20] Martí A and Luque A 1997 *Phys. Rev. Lett.* **78** 5014
[21] Li T, Bartolo R E and Dagenais M 2013 *Appl. Phys. Lett.* **103** 141113
[22] Martí A, Antolín E, Farmer C D, Linares P G, Hernández E, Sśnchez A M, Ben T, Molina S I, Stanley C R and Luque A 2010 *J. Appl. Phys.* **108** 064513
[23] Martí A and Luque A 2010 *Adv. Mater.* **22** 160
[24] Martí A, Antolín E, Stanley C R, Farmer C D, López E, Díaz P, Cánovas E, Linares P G and Luque A 2006 *Phys. Rev. Lett.* **97** 247701
[25] Nozawa T, Takagi H, Watanabe K and Arakawa Y 2015 *Nano Lett.* **15** 4483
[26] Raghavan S, Forman D, Hill P, Weisse-Bernstein N R, von Winckel G, Rotella P, Krishna S, Kennerly S W and Little J W 2004 *J. Appl. Phys.* **96** 1036
[27] Wu J, Makableh Y F M, Vasan R, Manasreh M O, Liang B, Reyner C J and Huffaker D L 2012 *Appl. Phys. Lett.* **100** 051907
[28] Adler F, Geiger M, Bauknecht A, Haase D, Ernst P, Dörnen A, Scholz F and Schweizer H 1998 *J. Appl. Phys.* **83** 1631
[29] Datas A, López E, Ramiro I, Antolín E, Martí A and Luque A 2015 *Phys. Rev. Lett.* **114** 157701
[30] Pal D and Towe E 2006 *Appl. Phys. Lett.* **88** 153109
[31] Heitz R, Veit M, Ledentsov N N, Hoffmann A and Bimberg D 1997 *Phys. Rev. B* **56** 10435
[32] Li S S and Xia J B 2000 *J. Appl. Phys.* **88** 7171
[33] Schmidt T and Lischka K 1992 *Phys. Rev. B* **45** 8989
[34] Steer M J, Mowbray D J, Tribe W R, Skolnick M S, Sturge M D, Hopkinson M, Cullis A G, Whitehouse C R and Murray R 1996 *Phys. Rev. B* **54** 17738
[35] Kapteyn C M A, Stier O, Heitz R, Grundmann M, Zakharov N D and Bimberg D 1999 *Phys. Rev. B* **60** 14265
[36] Paskov P P, Monemar B, Garcia J M, Schoenfeld W V and Petroff P M 2000 *Appl. Phys. Lett.* **77** 812
[37] Harrison J W and Hauser J R 1976 *J. Appl. Phys.* **47** 292
[38] Martí A, Luque A, Ramiroa I, Antolín E and Tobías I 2013 *Sol. Energy Mater. Sol. Cells* **115** 138
[39] Mellor A, Tobías I and Martí A 2014 *Adv. Funct. Mater.* **24** 339
[40] Sturge M D 1962 *Phys. Rev.* **127** 768
[41] Elliott R J 1957 *Phys. Rev.* **108** 1384